Ann. For. Res. 67(1): xx-xx, 2024
https://doi.org/10.15287/afr.2024.3664

**ANNALS OF FOREST RESEARCH**
www.afrjournal.org

# Integration of Terrestrial Laser Scanning and field measurements data for tree stem volume estimation: Exploring parametric and non-parametric modeling approaches

**Florin Capalb[1,2], Bogdan Apostol[1], Adrian Lorenț[1,2]✉, Marius Petrila[1], Cristiana Marcu[1], Nicolae Ovidiu Badea[1,2]**

**Capalb F., Apostol B., Lorenț A., Petrila M., Marcu C., Badea N.O.,** 2024. Integration of Terrestrial Laser Scanning and field measurements data for tree stem volume estimation: Exploring parametric and non-parametric modeling approaches. Ann. For. Res. 67(1): xx-xx.

**Abstract** Terrestrial laser scanning (TLS) has emerged as a powerful tool for acquiring detailed three-dimensional information about tree species. This study focuses on the development of models for tree volume estimation using TLS data for even aged *Fagus sylvatica* L. stands located in the western part of the Southern Carpathians, Romania. Both parametric and non-parametric modeling approaches were explored, leveraging variables extracted from TLS point clouds such as diameter at breast height (DBH), height, crown radius, and other relevant crown and height parameters. Reference data were collected through high-precision field measurements across 76 circular Permanent Sample Areas (PSA) spanning 500 $m^2$ each. A multi-scan approach was implemented for TLS data collection, involving four scanning stations within each PSA. Concurrently, parametric (regression equations) and non-parametric (Random Forest - RF) models were applied, leveraging all TLS-derived variables to explore potential enhancements in volume estimation accuracy. Among the parametric models, the most effective performer was the one featuring solely DBH as an input variable. The RF non-parametric model yielded more accurate stem volume estimates (RMSE = 1.52 $m^3$*0.1$ha^{-1}$; RRMSE = 3.62%; MAE = 1.22$m^3$*0.1$ha^{-1}$) compared to the best-performing regression model (RMSE = 5.24 $m^3$*0.1$ha^{-1}$; RRMSE = 12.48%; MAE = 4.28 $m^3$*0.1$ha^{-1}$). Both types of models identified DBH as the most important predictive variable, while the RF model also included height and crown related parameters among the variables of importance. Results demonstrate the effectiveness of the non-parametric RF model in providing accurate and robust estimates of tree stem volume within even aged European beech stands. The integration of these models in operational forestry can enhance precision in biomass estimation and forest resource management. Future studies should aim to validate these models across diverse forest ecosystems to further refine and enhance their applicability.

**Keywords:** Terrestrial Laser Scanning (TLS), tree volume assessment, Random Forest algorithm, parametric models.

**Addresses:** [1]National Institute for Research and Development in Forestry “Marin Drăcea”, Voluntari, Romania.| [2]Faculty of Silviculture and Forest Engineering, “Transilvania” University of Braşov, Brașov, Romania.

✉ **Corresponding Author:** Adrian Lorenț (adrian.lorent@icas.ro).

**Manuscript:** received May 1, 2024; revised June 6, 2024; accepted June 9, 2024.

## Introduction

Various remote sensing technologies and field survey instruments are currently being used for forest assessment at a fine scale so as the term precision forestry has emerged which can be defined as a method to accurately determine characteristics of forests and treatments at stand, sub-stand or individual tree level (Holopainen et al. 2014). The remote sensing technologies used in precision forestry generally refers to: high and very high multispectral satellite imagery, airborne and terrestrial laser scanning and unmanned aerial vehicles (UAVs) (Fardusi et al. 2017). Very high (< 1 m) and high (< 10 m) spatial resolution optical satellite imagery supports forest inventories tasks such as identifying dominant species, determination of stand height, volume and biomass estimation or basal area and crown closure (White et al. 2016). New digital aerial photogrammetry systems, used either with manned or unmanned aerial vehicles, have enabled the production of image-based point clouds (similar to the LiDAR points). The UAVs usage in collecting forest inventory attributes exploded in recent years, however, the UAVs derived point cloud are limited to characterizing the outer canopy envelope since the canopy penetration rate is limited (White et al. 2016) or it can be used in conjunction with airborne laser scanning data which will delivers accurate digital terrain models for the surveyed area.

The use of high-resolution three-dimensional (3D) point clouds derived from airborne laser scanning (ALS) as well as terrestrial laser scanning (TLS) is an area of intense research for characterizing forest ecosystems (Shang et al. 2019, Calders et al. 2020, Dobre et al. 2021). Despite advancements in remote sensing, gaps remain in integrating TLS data for comprehensive forest inventory (Disney et al. 2019, Niță et al. 2021, Wardius et al. 2024). This study addresses these gaps by comparing parametric and non-parametric models, thus contributing to more accurate forest biomass estimation and management practices.

ALS is an active remote sensing technology that measures the three-dimensional distribution of forest vegetation, suitable for describing the vertical structure of the forest (Smreček et al. 2018), capable of covering large areas in short periods of time and at relatively reduced costs (Shang et al. 2019). Although ALS systems are efficient in covering extensive areas, they encounter difficulties in accurately detecting ground-level forest vegetation. Even though it has a greater canopy penetration rate than the UAVs point cloud, the ALS point cloud cannot be used to directly measure the tree DBH. In this context, TLS stands out as a technology capable of obtaining detailed three-dimensional point clouds representation of the canopy as well as of the overstory (i.e. shrubs and low trees) and the near-ground vegetation (White et al. 2016), thus providing detailed information about forest structure (Pascual et al. 2019, Wang et al. 2021), particularly in the canopy gap zone (Zhou et al. 2023b).

The potential of TLS for forest monitoring was first highlighted in the early 2000s. Initially, applications were focused on measuring trees and their components, such as diameter at breast height (DBH) (Wezyk et al. 2007) and height (García et al. 2011), eventually evolving towards estimating tree volume (Pitkänen et al. 2021, Abegg et al. 2023), aiming to improve above-ground biomass (AGB) determination (Liang et al. 2016, Demol et al. 2021, Demol et al. 2022). Thus, TLS-derived data are used to obtain information about dendrometric characteristics of trees and stands (Zhong et al. 2017, Cabo et al. 2018), as well as detailed data on stand structure (Lim et al. 2003, Burt et al. 2013, Åkerblom & Kaitaniemi 2021), thereby contributing to efficient forest resource management (Moskal & Zheng 2012, Rehush et al. 2018, Oruç & Öztürk 2021, Wilson et al. 2021).

TLS can be used as a complementary system to ALS, considering its ability to observe the canopy structure from below the canopy upwards from a radial perspective, while ALS observes the canopy from top, down, almost exclusively at close to nadir view (White et al. 2016).

In previous research, TLS has been used to estimate dendrometric characteristics of trees, focusing particularly on estimating DBH, tree height, crown dimensions, as well as tree positioning (Maas et al. 2008, Olofsson et al. 2014, Srinivasan et al. 2015, Bienert et al. 2018, Bogdanovich et al. 2021). This information has been utilized in both trunk segmentation (Li et al. 2020), volume estimation (Saarinen et al. 2017), and determination of the three-dimensional crown structure (Zhu et al. 2020, Han & Sánchez-Azofeifa 2022).

Thus, the use of TLS has shown great potential for estimating the volume of trees and stands, with two approaches to accomplish this. In the first approach, volume is determined using TLS data obtained through geometric reconstruction of trees (Abegg et al. 2023). Another approach for tree volume estimation involves applying regression equations based on dendrometric characteristics of single trees extracted from point cloud segmentation (Mayamanikandan et al. 2019, Pitkänen et al. 2021).

In this context, the selection and optimization of models, as well as considering a larger number of factorial variables (such as crown dimensions, knot-free height, stand structure, age, site conditions, etc.) in the process of estimating tree and stand volume, represent important steps in the foundation of these models. For instance, the study conducted by Popescu et al. 2003 highlighted the importance of crown diameter, determined from point clouds, in estimating tree volume, while (Iizuka et al. 2020) found that the best result in estimating the stem volume from remote sensing data was obtained using canopy height, canopy size and canopy cover as input variables.

In the context of tree volume estimation, traditional models are generally linear, non-linear, or mixed-effects models. These models often require meeting statistical assumptions such as data independence, normal distribution, and equal variance to be properly applied. However, an alternative approach to tree volume estimation involves using models based on the Random Forest (RF) algorithm. Indeed, these models enable a more efficient estimation of nonlinear relationships without imposing a specific data structure, in contrast to parametric models that assume certain distributions or functional relationships between variables. This provides increased flexibility in adapting the models to observed data, RF models being capable of capturing complex and non-linear relationships between input variables and their outcomes, in particular, it can deal with clustered data, as well as missing data (Auret & Aldrich, 2012). Additionally, RF models are not limited by issues associated with covariance and unequal data variability, making them an attractive option in tree volume estimation.

Previous studies have demonstrated that RF models have a higher potential for estimating tree volume compared to traditional models, primarily being applied for estimating stand volume and biomass on a large scale (Silva et al. 2017, Esteban et al. 2019).

The selection and optimization of models for estimating tree volume are crucial aspects in improving these estimations. Models based on the RF algorithm have demonstrated better potential in estimating tree volume compared to traditional models, providing flexibility in adapting to observed data and avoiding issues associated with unequal data variability (Wang et al. 2023).

The RF algorithm is known for its ability to efficiently handle data with unequal variability, as well as for its capability to provide robust estimates. This is because RF is a combination of multiple individual decision trees, and the final result is obtained as an average of their predictions.

In the context of estimating tree volume, the use of the RF algorithm allows for the exploration and integration of a large number of features and variables. This facilitates obtaining precise and robust volume estimates, considering the diversity and complexity of the data involved in the estimation process.

Within this context, the aim of this study is to investigate the potential of employing TLS data for developing volume models tailored to individual trees. The main objective was to conduct a comparative analysis between individual tree volumes calculated from field data and those estimated from TLS point cloud processing, using specific parametric and non-parametric models.

## Materials and methods

The study site is situated in Romania, within the western region of the Southern Carpathians, specifically within the northwestern section of the Retezat-Godeanu mountain range, notably within the Tarcu Mountains in the Muntele Mic district. It spans the upper basin of the Sebeș River, encompassing the main valleys of Cuntu and Valea Craiului, with peak elevations surpassing 2100 meters (Figure 1).

In the year 2020, according to a specific methodology (Badea 2013), a total of 38 Permanent Plots (PP) were inventoried in a systematic network, sized according to the dominant tree species (i.e. *Fagus sylvatica* L.) and stands age. Each PP comprises two circular Permanent Sample Areas (PSA), each with a radius of 12.62 meters, covering an area of 500 m$^2$. Thus, in total there were inventoried trees within 76 PSAs.These PSAs are positioned at a distance of 30 meters from the center of the PP (Figure 2). On flat terrain, the PSAs are oriented towards each other in the east-west direction, while on inclined terrain, they are aligned along the contour line. The sizing of the network, including determining the number of plots and the distance between them, was carried out using information regarding the coefficients of variation of volume calculated based on data from U.P. VI - Cuntu management plan of B.E. Caransebeș, 2016 edition (Cojoacă 2016).

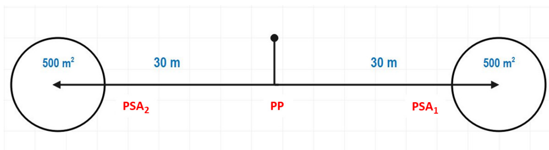


**Figure 2** The positioning of the permanent sample area (PSA) in relation to the center of the permanent plots (PP).

The coordinates of the centers of the PPs and PSAs were recorded using a Trimble GeoXH device equipped with a Zephir II antenna and were marked using metal stakes (20 cm) completely buried in the ground, as well as wooden markers (stakes) with the upper end approximately 30 cm above the ground, highlighted with white paint. Within the PSA, all trees with a DBH equal, or greater than 6 cm were inventoried, and their descriptive information was recorded using the FieldMap equipment (Petrila et al. 2012). The characteristics determined, measured, or estimated during the inventory included: tree position, DBH, species, tree height (h), pruned height, crown projection, Kraft class, and descriptive information


**Figure 1** Research area location map (base map – digital elevation model from Shuttle Radar Topography Mission (SRTM).

such as tree vitality. The DBHs were measured using a forest caliper, while heights were measured using the Vertex IV instrument.

To compute the reference aboveground volume of each tree, we utilized a specific equation (Giurgiu et al. 2004) (Eq. 1), commonly applied for forest tree species in Romania:

$$\mathbf{log}\, v = a_0 + a_1\, \mathbf{log}\, d + a_2\, \mathbf{log^2}\, d + a_3\, \mathbf{log}\, h + a_4\, \mathbf{log^2}\, h, \quad \text{(Eq. 1)}$$

where $d$ represents the tree's diameter at breast height, in cm; $h$ – tree height, in m; $v$ – volume of the tree, in m$^3$; $a_0$ - $a_4$ – regression coefficients, established by species (Giurgiu et al. 2004).

Within the PSAs specific measurements were conducted using a static terrestrial laser scanner, namely the FARO 3D X130 HDR model (Figure 3). This high-precision device has a distance estimation error of ±2 mm at 25 m and a laser wavelength of 1550 nm (FARO Technologies Inc 2019).

To ensure data accuracy and a high level of detail, a multiple scan approach of each PSA was conducted. Additionally, to ensure precise co-registration of the point clouds resulting from the terrestrial scanning, seven spherical markers were uniformly placed in each PSA.

The main advantage of using multiple scans from different directions compared to a single scan placed at the center of the PSA lies in identifying a higher number of trees. This aspect has a direct impact on the precision of estimating dendrometric parameters of trees (Apostol et al. 2018) because it allows covering a larger area and obtaining a more complete representation of the forest environment. Consequently, multiple scans provide a more detailed 3D representation of the trees in the PSA, including their crowns and branches, facilitating a more precise estimation of DBH. Thus, within each PSA, TLS measurements were conducted by establishing four stations. The first station was placed at the center of the PSA, the second towards the north direction, the third at 120º from the north direction, and the last one at 240º. The TLS stations, except for the one placed at the center of the PSA, were positioned at a distance of 15 meters from the center of the PSA (Figure 4). While the systematic network of PSAs ensures broad coverage, potential biases due to site accessibility and forest structure variability must be considered. Additionally, the precision of TLS equipment and the complexity of data processing may limit the generalizability of findings.

To achieve automatic co-registration of the TLS point clouds it was necessary to place spherical targets uniformly within the PSA. Subsequently, the obtained data were input into the TLS dedicated software (FARO Technologies Inc, 2019) for primary processing and to generate a single point cloud corresponding to each PSA, and exported in .LAS file format, which allows further processing.

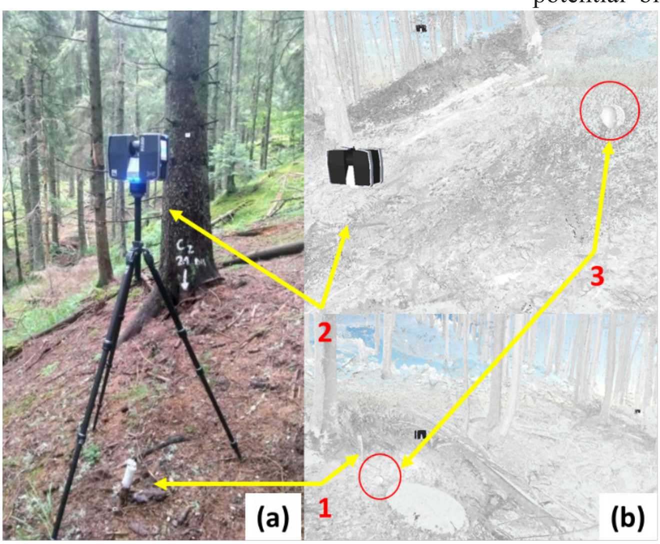


**Figure 3** The terrestrial laser scanning device positioned at the center of a permanent sample area (PSA): (1) PSA center; (2) TLS position; (3) Spherical reference point; (a) photo captured in the field; (b) TLS point cloud co-registered using Scene software.

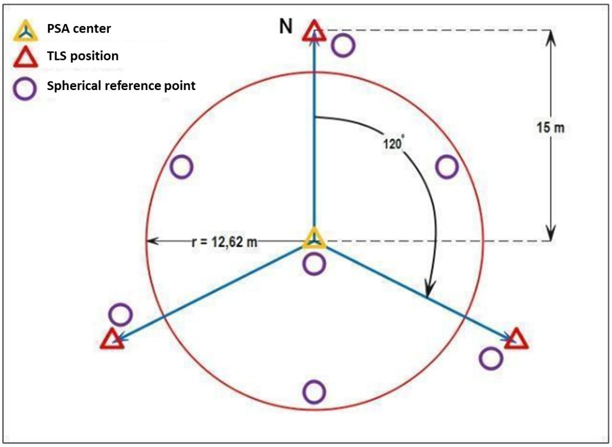


**Figure 4** Data acquisition with terrestrial laser scanning within the permanent sample area (PSA)

The dimensional characteristics of the crown, such as the maximum crown radius (Cr), crown length (CL), as well as its volume, were derived from the point cloud using the TreeLS (de Conto et al. 2017, R Core Team 2021) and VoxR packages implemented in R software (Lecigne et al. 2018; R Core Team 2021). The DBH was extracted using the IRLS algorithm (Liang et al. 2012) implemented in the TreeLS package (de Conto et al. 2017), as well as through the use of the FORTLS package (Molina-Valero et al. 2022), developed to automate the processing of TLS point cloud data and to estimate forest variables. Tree heights were determined through semantic segmentation of the point cloud, identifying the tree crown top, which corresponds to the maximum height recorded within the point cloud at that position (de Conto et al. 2017, Molina-Valero et al. 2022). However, due to the significant errors associated with determining tree height using TLS, often resulting in underestimation (Apostol et al. 2018, Pascu et al. 2020, Wardius & Hein 2024), the heights derived from TLS were not utilized in the development of tree stem volume models, except for the pruned height (Hrv). Instead, height metrics (i.e. Hp50, Hiq, Hstd, Hp01) were calculated at the level of PSA from the heights of segmented semantic tree cylinders.

In the development of models to estimate tree stem volume using TLS data, the selection of appropriate variables is crucial for achieving precise and dependable results. Within this context, the utilization of parametric and non-parametric models represents two distinct approaches, each offering unique advantages and applications.

In this study, we examined both, parametric models - which depend on predefined functional relationships between independent variables and outcomes, and the Random Forest (RF) - non-parametric model that has the capability to capture complex and nonlinear relationships between variables. The variable selection for each model considered the significance and relevance of these factors in estimating tree stem volume. The chosen variables were selected for their significant impact on tree stem volume estimation and their potential to enhance the model's accuracy (Giurgiu 1979).

After the semantic segmentation of TLS point clouds, the following data were computed as independent variables: DBH, pruned height (Hrv), height at which 50% of the total trees are found (Hp50), height at which 1% of the total trees are found (Hp01), crown volume (Vc), crown length (CL), ratio of crown length to pruned height (CLr), standard deviation of height (Hstd), maximum crown radius (Cr), interquartile height range (Hiq) and maximum crown radius (Cr) . These variables were used in the development of four parametric models:

-Model 1: includes DBH as the only independent variable.

-Model 2: includes as independent variables: DBH, pruned height (Hrv), height at which 50% of the total trees are found (Hp50) and interquartile height range (Hiq).

-Model 3: includes as independent variables: DBH and crown length (CL), and the ratio of crown length to pruned height (CLr).

-Model 4: includes as independent variables: DBH, crown volume (Vc), maximum crown radius (Cr), height at which 50% of the total trees are found (Hp50), height at which 1% of the total trees are found (Hp01) and standard deviation of height (Hstd).

Within the non-parametric modeling approach for tree volume estimation, we investigated the utilization of Random Forest (RF) model.

In the application of the RF algorithm, we explored the diverse effects of the number of decision trees and the selection of variables considered at each split. We examined a broad range, spanning from 50 to 250 decision trees, to evaluate how this aspect influences model performance. Additionally, we tested different numbers of variables for each split, ranging from 2 to 6, to discern how this factor contributes to model improvement.

The RF algorithm allows determining this relative importance and generates a partial dependence plot for the dependent variable (Schonlau & Zou 2020), which is essential for improving RF results.

To substantiate the methodology of estimating tree volume, the dataset containing the identified trees from point cloud processing (TLS) was randomly partitioned. Seventy-five percent of the total identified trees were allocated for training the parametric models and RF algorithm, while the remaining 25% were reserved for validation (testing).

The evaluation of the prediction abilities of both parametric models and the RF algorithm was carried out using the coefficient of determination ($R^2$) (Eq. 2), root mean square error (RMSE) (Eq. 3), relative root mean square error (RRMSE) (Eq. 4), and mean absolute error (MAE) (Eq. 5). These metrics were utilized to compare the predicted stem volume of each parametric and non-parametric approach with the field reference tree stem volume calculated using specific methods (Giurgiu et al. 2004). The same metrics were then determined at the plot (PP) level for the best performing parametric model and the RF non-parametric model. Plot level stem volumes were obtained by summing the individual stem volumes calculated through the parametric and non-parametric methods, respectively

$$R^2 = 1 - \left[\frac{\sum_{i=1}^{n}(y_i - \hat{y}_i)^2}{\sum_{i=1}^{n}\left(y_i - \underline{y_i}\right)^2}\right] \quad \text{(Eq. 2)}$$

$$RMSE = \sqrt{\frac{\sum_{i=1}^{n}(y_i - \hat{y}_i)^2}{n}} \quad \text{(Eq. 3)}$$

$$RRMSE = \frac{\sqrt{\frac{\sum_{i=1}^{n}(y_i - \hat{y}_i)^2}{n}}}{\sum_{i=1}^{n} y} * 100 \quad \text{(Eq. 4)}$$

$$MAE = \sum_{i=1}^{n}\left|\frac{y_i - \hat{y}_i}{y_i}\right| \quad \text{(Eq. 5)}$$

where n is the number of observations, $y_i$ is the observed value, $\hat{y}_i$ is the predicted value, and $\bar{y}$ is the arithmetic mean of observed values.

The entire workflow adopted to estimate tree stem volume is organized into three distinct stages (Figure 5).

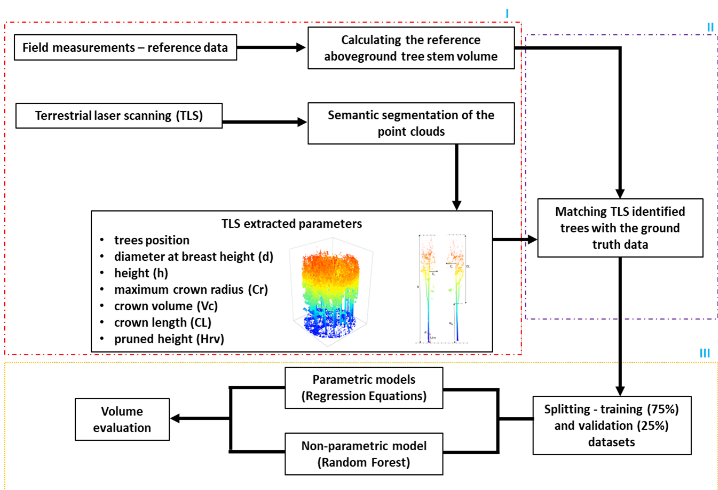


**Figure 5** The workflow of the study methodology.

## Results

Following the inventories conducted in 2020, 38 PPs, corresponding to 76 PSAs, where a total of 2924 trees were identified and measured (Figure 6). Furthermore, in 2021, all plots underwent comprehensive surveying and scanning using terrestrial laser scanning, resulting in a total of 304 scans. Subsequent to processing the point clouds, statistical reports were generated for each permanent sampling plot, providing insights into the accuracy of co-registration. As a result, the collation of these reports revealed an average co-registration error of 7.1 mm (Table 1). Among all permanent sampling plots, roughly 90% exhibit an average co-registration error of less than 10 mm. Furthermore, 97% of the plots meet the acceptable tolerances for determining dendrometric parameters (<20 mm), with the exceptions being PSAs 732 and 741.

The result of semantic processing of point clouds obtained from terrestrial laser scanning is represented in the form of three-dimensional point clouds (Figure 7), with high density, having attributes such as spatial coordinates (X, Y, Z) of each point, as well as information regarding their classification into four classes: points classified as ground (Figure 8a), points classified as forest vegetation (tree crowns) (Figure 8b), points classified as tree trunks and thick branches (Figure 8c), and points classified as dead wood on the ground (Figure 8d).

Following the point cloud segmentation, variables such as tree DBH (d), height of segmented semantic tree cylinder (h), pruned height (Hrv), maximum crown radius (Cr), crown volume (Vc), and crown length (CL) variables were extracted (Figure 9). Additionally, height metrics, such as height at which 50% of the total trees are found (Hp50), interquartile height range (Hiq), standard deviation of height (Hstd) and height at which 1% of the total trees are found (Hp01) were calculated from the heights of segmented semantic tree cylinders. Furthermore, the ratio between crown length (CL) and pruned height (Hrv) was calculated using the aforementioned data. These details allowed for a comprehensive characterization of individual trees and

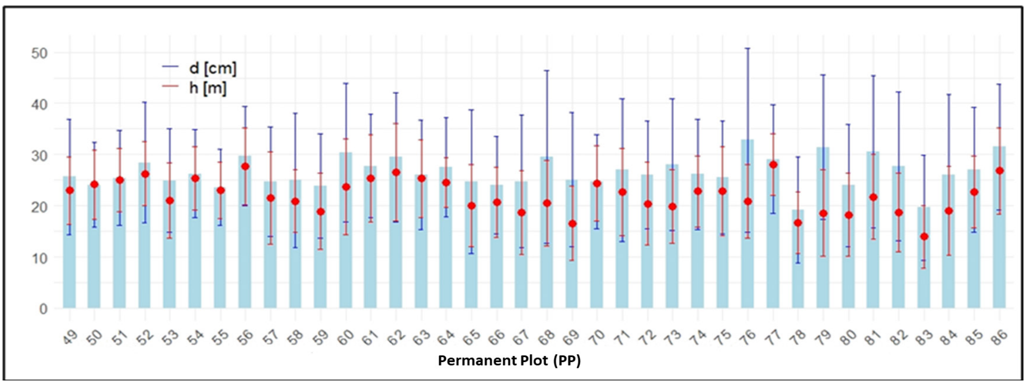


**Figure 6** Distribution of mean diameter and mean height determined at PP level.

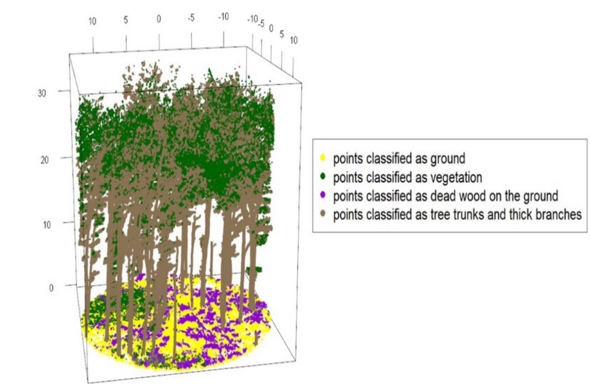


**Figure 7** The three-dimensional point cloud resulting for a PSA.

**Table 1** Co-registration accuracy determined for permanent sample area (PSA).

| Permanent Sample Area (PSA ID number) | Maximum Point Error (mm) | Mean Point Error (mm) | Minimum Overlap (%) | Code of Permanent Sample Area (PSA ID number) | Maximum Point Error (mm) | Mean Point Error (mm) | Minimum Overlap (%) |
|---|---|---|---|---|---|---|---|
| 491 | 6.9 | 6.9 | 54.2 | 681 | 7.0 | 5.9 | 27.6 |
| 492 | 7.3 | 6.2 | 34.1 | 682 | 5.0 | 4.8 | 23.6 |
| 501 | 14 | 12.7 | 35.9 | 691 | 5.8 | 5.1 | 46.8 |
| 502 | 5.3 | 4.1 | 35.4 | 692 | 6.2 | 5.8 | 38.4 |
| 511 | 5.9 | 4.7 | 34.8 | 701 | 7.4 | 5.4 | 30.3 |
| 512 | 6.5 | 5.2 | 43.0 | 702 | 9.6 | 7.3 | 22.4 |
| 521 | 4.7 | 3.7 | 31.4 | 711 | 11.3 | 9.2 | 30.5 |
| 522 | 6.1 | 5.1 | 32.0 | 712 | 11.6 | 8.6 | 22.5 |
| 531 | 7.7 | 5.7 | 33.8 | 721 | 7.7 | 6.6 | 29.3 |
| 532 | 7.5 | 6.5 | 29.4 | 722 | 8.2 | 6.7 | 38.6 |
| 541 | 5.9 | 4.7 | 33.2 | 731 | 9.8 | 7.5 | 34.0 |
| 542 | 5.5 | 4.5 | 39.7 | 732 | 32.2 | 20.5 | 24.5 |
| 551 | 6.5 | 5.0 | 28.9 | 741 | 30.4 | 22.7 | 23.2 |
| 552 | 6.4 | 4.8 | 38.0 | 742 | 6.9 | 6.1 | 43.7 |
| 561 | 6.7 | 5.3 | 41.7 | 751 | 13.3 | 8.6 | 26.9 |
| 562 | 8.4 | 6.7 | 24.3 | 752 | 6.7 | 5.9 | 39.0 |
| 571 | 5.7 | 4.8 | 36.7 | 761 | 11.1 | 9.2 | 33.1 |
| 572 | 6.6 | 5.1 | 32.5 | 762 | 8.2 | 7.6 | 31.3 |
| 581 | 5.9 | 5.1 | 44.9 | 771 | 10.2 | 8.3 | 31.9 |
| 582 | 8.1 | 6.3 | 35.1 | 772 | 7.9 | 6.0 | 36.2 |
| 591 | 9.4 | 9.4 | 33.1 | 781 | 7.1 | 6.2 | 38.2 |
| 592 | 26.3 | 16 | 25.9 | 782 | 8.9 | 7.6 | 37.3 |
| 601 | 5.7 | 4.7 | 36.8 | 791 | 9.4 | 7.3 | 25.6 |
| 602 | 4.9 | 3.8 | 28.0 | 792 | 9.4 | 7.7 | 40.5 |
| 611 | 10.2 | 6.9 | 28.1 | 801 | 6.6 | 6.2 | 33.9 |
| 612 | 6.1 | 4.8 | 32.8 | 802 | 15.4 | 10.9 | 7.2 |
| 621 | 9.9 | 6.4 | 32.9 | 811 | 6.8 | 6.3 | 28.9 |
| 622 | 7.2 | 5.8 | 28.1 | 812 | 6.2 | 5.3 | 38 |
| 631 | 9.6 | 7.3 | 35.6 | 821 | 6.9 | 6.2 | 41.2 |
| 632 | 8.6 | 5.7 | 34.1 | 822 | 6.7 | 5.5 | 32.5 |
| 641 | 12.8 | 9.7 | 34.3 | 831 | 13.7 | 9.9 | 31 |
| 642 | 12.2 | 10.5 | 30.5 | 832 | 10.0 | 7.9 | 33 |
| 651 | 11.1 | 8.9 | 37.7 | 841 | 6.1 | 5.5 | 38.8 |
| 652 | 11.3 | 9.3 | 33.8 | 842 | 5.8 | 5.1 | 36.6 |
| 661 | 8.6 | 7.9 | 27.8 | 851 | 5.9 | 4.5 | 35.8 |
| 662 | 25 | 15 | 24.4 | 852 | 6.2 | 4.5 | 44.5 |
| 671 | 7.8 | 7.3 | 43.1 | 861 | 4.3 | 3.6 | 38.6 |
| 672 | 7.5 | 7.5 | 27.8 | 862 | 6.6 | 4.7 | 41.1 |

| Mean of Maximum Point Error (mm) | Mean of Mean Point Error (mm) | Mean of Minimum Overlap (%) |
|---|---|---|
| **9.1** | **7.1** | **33.6** |

their crowns, providing a deeper understanding of their structure and dimensions.

Following the processing of TLS point clouds a total of 2596 trees were identified from 38 permanent plots (PP) based on the position of the trees. Thus, according to the confusion matrix (Table 2), a total of 1881 trees were accurately matched with the reference dataset. This yields an accuracy of 55.6% (the ratio of correctly correlated trees to the total number of trees) and a precision of 72.4% (the ratio of correctly correlated trees to the total number of trees identified from the processing of point clouds).

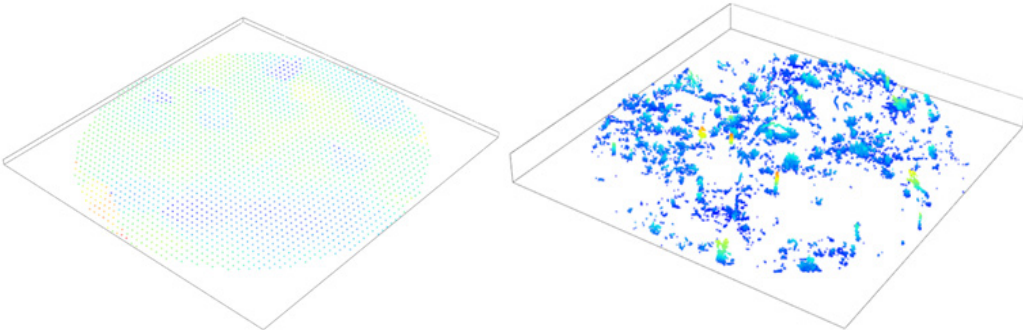

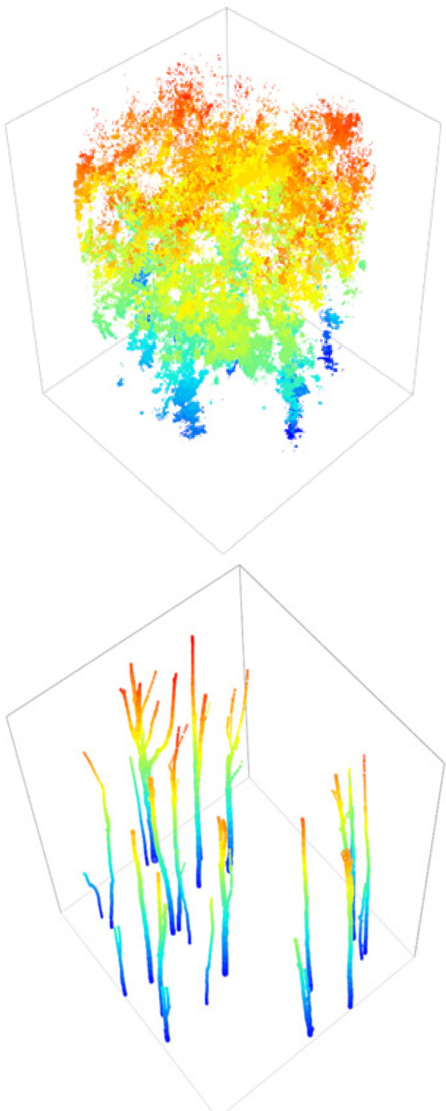

**Figure 8** Semantic segmented point cloud: (a) points classified as ground; (b) points classified as forest vegetation; (c) points classified as tree trunks and thick branches; (d) points classified as dead wood on the ground.

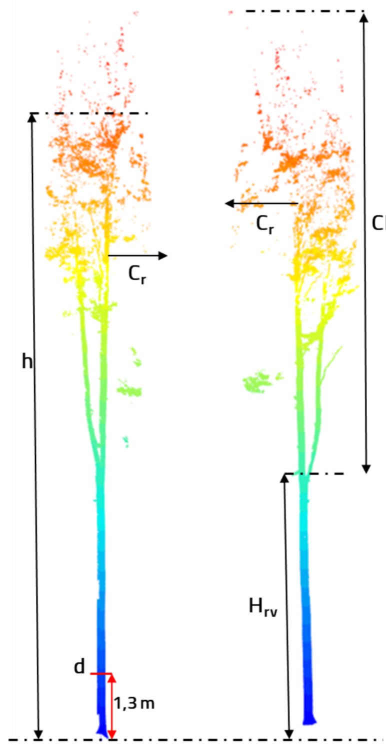


**Figure 9** The structure of the data extracted from semantic segmentation of TLS point clouds. d – DBH; h – height of segmented semantic tree cylinder; Cr – maximum crown radius; CL – crown length; Hrv – pruned height.

However, 328 trees existing in the field were not identified in the TLS data. Furthermore, a total of 715 trees were exclusively identified in the dataset resulting from terrestrial laser scanning and did not have a counterpart in the reference dataset.

Additionally, from the field data, a total of 1043 trees could not be identified; however, 19% of these are trees that are forked at the base (54 trees), dead (89 trees), and that are either bent or have a broken trunk (56 trees).

The analysis of the four parametric models, developed based on the selection of TLS-based extracted variables, indicates that Model 1 emerges as the optimal parametric model for estimating tree stem volume (Table 3). This determination is corroborated by the values of $R^2$ = 0.92, RMSE = 0.26 $m^3$, MAE = 0.16 $m^3$, and RRMSE = 30%.

**Table 2** Confusion matrix for the TLS identified trees and field reference trees.

| | TLS identified trees | |
|---|---|---|
| | **TN** | **FP** |
| Reference trees | 328 | 715 |
| | **FN** | **TP** |
| | 1043 | 1881 |

Note: TP - corresponding trees,identified both through field inventories and TLS point cloud processing; TN - trees existing in the field but not identified through TLS point cloud processing; FP - trees identified through TLS point cloud processing but not corresponding to field data; FN - trees existing in the field for which correspondence could be established with trees identified through TLS point cloud processing

When estimating tree stem volume using the RF algorithm, the relative importance of variables extracted from the semantic segmentation of TLS point clouds was assessed. It was observed that the DBH emerged as the most influential variable, with a relative importance (IncMSE%) (Figure 10) of approximately 60% in decreasing the root mean square error. This underscores the substantial impact that DBH has on the model's accuracy.

Furthermore, through testing various configurations of variables and numbers of decision trees used by the RF algorithm, it

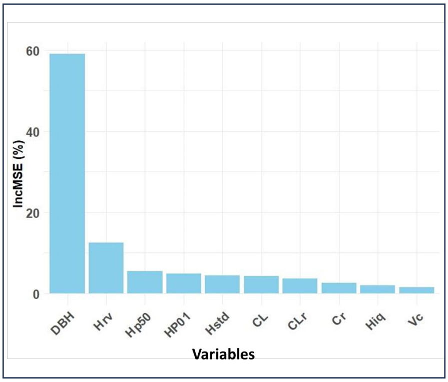


**Figure 10** Relative importance of the independent variables in the RF model.

**Table 3** Tree volume assessment based on parametric models.

| Variables | Models | | Train data | | | | Test data | | | | Total number of trees | | | |
|---|---|---|---|---|---|---|---|---|---|---|---|---|---|---|
| | | | $R^2$ | RMSE ($m^3$) | MAE ($m^3$) | RRMSE (%) | $R^2$ | RMSE ($m^3$) | MAE ($m^3$) | RRMSE (%) | $R^2$ | RMSE ($m^3$) | MAE ($m^3$) | RRMSE (%) |
| DBH (d) | M1 | v | 0.90 | 0.27 | 0.17 | 30 | 0.88 | 0.21 | 0.14 | 29 | 0.92 | 0.26 | 0.16 | 30 |
| DBH(d) and height variables | M2 | v | 0.70 | 0.45 | 0.42 | 35 | 0.65 | 0.48 | 0.31 | 39 | 0.77 | 0.42 | 0.28 | 44 |
| DBH (d) and crown variables | M3 | v | 0.85 | 0.38 | 0.38 | 42 | 0.71 | 0.46 | 0.28 | 40 | 0.83 | 0.36 | 0.24 | 42 |
| DBH (d), height and crown variables | M4 | v | 0.85 | 0.52 | 0.20 | 37 | 0.75 | 0.42 | 0.18 | 34 | 0.86 | 0.38 | 0.25 | 36 |

Note: v - tree stem volume, $m^3$; d - DBH, cm; Hrv - pruned height, m; Hp50 - height at which 50% of total trees are located, m; Hp01 - height at which 1% of total trees are located, m; Hstd - standard deviation of height, m; CL - crown length, m; CLr - ratio of crown length to pruned height; Cr - maximum crown radius, m; Hiq - interquartile height range, m; Vc - crown volume, $m^3$. M1: $v = 0,2653 - 0,0292*d + 0,0017*d^2$; M2: $v = 0,0720*d - 0,0044*H_{rv} - 0,0422*H_{p5} - 0,0404*H_{iq}$; M3: $v = 0,0779*d + 0,0101*CL - 0,0152*CLr - 1,3174$; M4: $v = -0,0421*d - 0,0198*H_{p50} + 0,1494*H_{p01} + 0,0649*H_{std} + 0,1634*C_r - 0,0001*V_c + 0,1376$.

was determined that employing 250 decision trees and considering 6 variables at each split led to a noteworthy reduction in estimation error and a substantial improvement in model performance. Hence, the results illustrated that augmenting the number of variables considered at each split and increasing the number of decision trees positively influenced the performance of the RF algorithm. For instance, when the RF algorithm was tested with only 2 variables, the mean squared error (MSE) was 0.084. However, for the model with 6 variables, this error was reduced to below 0.018 (Figure 11).

Comparing the tree stem volume estimated by the best-performing parametric model (Model 1) with that estimated by the non-parametric model using the RF algorithm reveals that the inclusion of supplementary variables and the adoption of a non-parametric approach enhance the accuracy of volume estimation. This is evidenced by an increase $R^2$ by approximately 6%, indicating better explainability of the variation in the data; a decrease RMSE by approximately 37%, and RRMSE by 52 % reflecting higher precision in volume estimation; and a reduction in MAE by approximately 50% (Table 4). The RF model's superior performance, indicated by a 52% reduction in RRMSE compared to the best parametric model, underscores its potential for improving operational forestry practices. These results highlight the importance of including crown parameters alongside DBH in volume estimation models.

**Table 4** Evaluation of the prediction abilities of the tree stem volume estimation based on parametric model 1 and non-parametric RF model.

| Model | Data | $R^2$ | RMSE ($m^3$) | MAE ($m^3$) | RRMSE (%) |
|---|---|---|---|---|---|
| Parametric model **(M1)** *(v ~ d)* | Train data | 0.90 | 0.27 | 0.17 | 30 |
| | Test data | 0.88 | 0.22 | 0.14 | 29 |
| | Total number of trees | 0.92 | 0.26 | 0.16 | 30 |
| Non-parametric model **RF** *(v ~ d, Hrv, Hp50, Hp01, Hstd, CL,CLr, Cr, Hiq, Vc )* | Train data | 0.98 | 0.12 | 0.06 | 17 |
| | Test data | 0.90 | 0.20 | 0.13 | 19 |
| | Total number of trees | 0.97 | 0.15 | 0.08 | 14 |

Note: v - tree stem volume, $m^3$; d - DBH, cm; Hrv - pruned height, m; Hp50 - height at which 50% of total trees are located, m; Hp01 - height at which 1% of total trees are located, m; Hstd - standard deviation of height, m; CL - crown length, m; CLr - ratio of crown length to pruned height; Cr - maximum crown radius, m; Hiq - interquartile height range, m; Vc - crown volume, $m^3$.

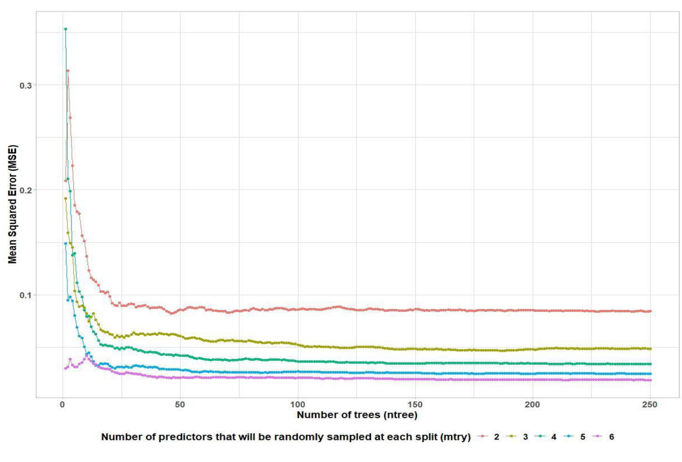


**Figure 11** Mean square error according to various configurations of variables and numbers of decision trees used by the RF algorithm.

Comparing the tree stem volume estimated by the best-performing parametric model (Model 1) with the field reference tree stem volume, we achieved an RMSE value of 0.26 m³. This value equates to approximately 30% of the average volume of the corresponding trees (RRMSE = 30%) (Figure 12a).

When comparing the total tree volume calculated at the PP level using field measurement data to the volume determined by the best-performing parametric model (Model 1), a strong and significant correlation between the two sets of values (r = 0.932**) was observed. However, despite this strong correlation, the analysis yielded an RMSE value of 5.24

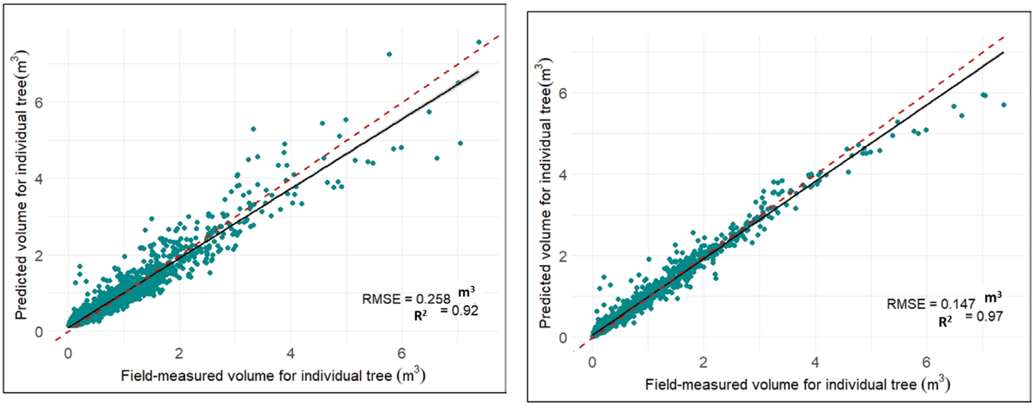


**Figure 12** Tree volume of reference compared to the estimated tree volume resulting from the semantic segmentation of point clouds for (a) parametric model M1, (b) RF non-parametric model .

$m^3$*0.1ha$^{-1}$, accompanied by an RRMSE of 12.5% and a MAE of 4.28 $m^3$*0.1ha$^{-1}$ (Figure 13a).

Furthermore, when comparing the tree stem volume estimated by the non-parametric model employing the RF algorithm with the field reference tree stem volume, we achieved an RMSE value of 0.147 $m^3$. This value equates to approximately 14% of the average volume of the corresponding trees (RRMSE = 14%). These results suggest a strong alignment between the estimated and measured values of the tree stem volume, indicating a robust fit of the model (Figure 12b).

When comparing the total tree volume calculated at the PP level using field measurement data to the volume determined by the non-parametric model, a strong and significant correlation between the two sets of values (r = 0.994**) was observed. However, despite this strong correlation, the analysis yielded an RMSE value of 1.52 $m^3$*0.1ha$^{-1}$, accompanied by an RRMSE of 3.62% and a MAE of 1.22 $m^3$*0.1ha$^{-1}$ (Figure 13b).

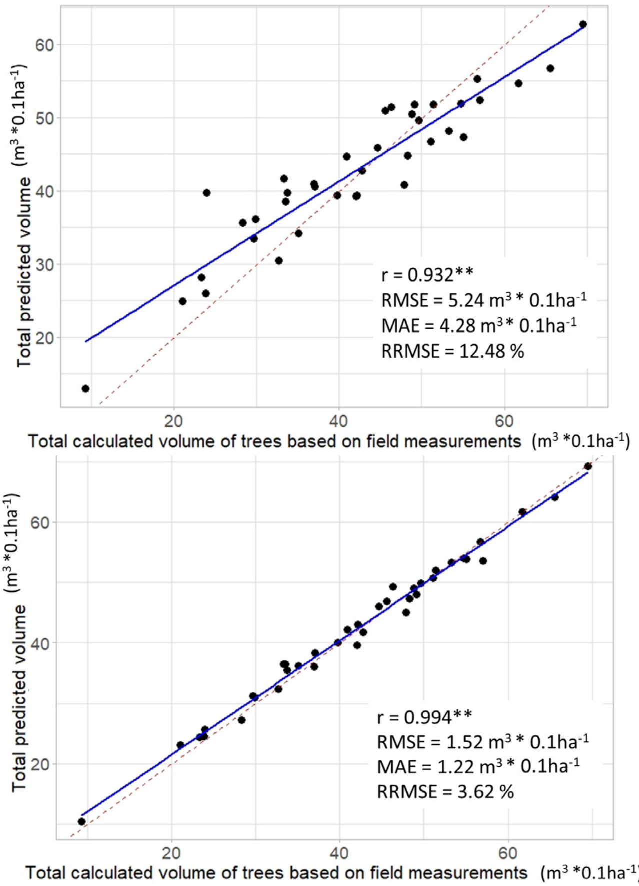


**Figure 13** The total volume of trees at PP level calculated based on the processing of TLS point clouds in relation to the volume of trees determined based on field measurements for (a) parametric model M1, (b) RF non-parametric model.

## Discussion

The use of TLS data for estimating forest variables such as DBH, tree height, and tree volume is a subject of significant interest to both the forestry community and forestry practice. When estimating tree volume based on TLS data, various approaches have been explored (Momo Takoudjou et al. 2018, Mayamanikandan et al. 2019, Brede et al. 2022, Singh et al. 2022). These include using allometric equations using tree DBH and height extracted from the TLS point cloud. Another approach involves using quantitative structure modeling technique (QSM), where volume is directly estimated from the TLS point cloud. In a study conducted by Momo Takoudjou et al. in 2018, they emphasized that tree volumes in semi-deciduous forests of eastern Cameroon, extracted from TLS data using the QSM technique, exhibit high precision ($R^2$ above 0.98 and RRMSE below 2.81%). In our study, we achieved comparable accuracy in tree volume estimation ($R^2$=0.98 and RRMSE=3.62%) using the non-parametric RF-based model. Another study (Brede et al. 2022), conducted across various test sites, including a beech forest in the Netherlands, highlights a lower coefficient of determination for tree volume estimation achieved through the QSM technique ($R^2$ =0.86) compared to the one obtained in our study ($R^2$ =0.98).

Traditional linear regression models, and more recently, machine learning-based methods applied to TLS data, have demonstrated their utility in modeling complex nonlinear allometric relationships between tree's variables (Aguilar et al. 2021, Wagers et al. 2021, Yrttimaa et al. 2022, Stovall et al. 2023).

Our findings underscore the efficacy of both parametric and non-parametric models in estimation tree stem volume using TLS data. Among the parametric approaches, Model 1, utilizing tree DBH as the sole independent variable extracted from TLS data, demonstrated the highest precision, with an RMSE of 5.24 $m^3$*0.1$ha^{-1}$ and an RRMSE of 12.48% at PP level. Conversely, the parametric Model 2, which integrates 3 supplementary parameters among one extracted as individual tree variable (i.e. Hrv) and two calculated at plot level (i.e. Hp50, Hiq) yielded the weakest performance. Notably, the RF non-parametric model, which integrates DBH with height (i.e. Hrv, Hp50, Hp01, Hiq, Hstd) and crown related variables (i.e. CL, CLr, Cr, Vc), outperformed the best performing parametric model in volume estimates both at tree level (RMSE = 0.15 $m^3$, RRMSE = 14%, MAE = 0.08$m^3$) and at PP level (RMSE = 1.52 $m^3$*0.1$ha^{-1}$, RRMSE = 3.62%, MAE=1.22$m^3$*0.1$ha^{-1}$) compared to the best performing regression model (M1) (RMSE = 0.26 $m^3$, RRMSE = 30%, MAE = 0.16$m^3$ at tree level; RMSE = 5.24 $m^3$*0.1$ha^{-1}$, RRMSE = 12.48%, MAE= 4.28 $m^3$*0.1$ha^{-1}$ at PP level), highlighting the effectiveness of RF non-parametric algorithm in the estimation of timber volume.

A limitation of our study arose from the inability to accurately extract tree heights from the TLS point cloud. Despite implementing a multiscan approach, the tops of the dominant trees were not consistently captured, leading to the underestimation of heights. Additionally, in the case of understory trees, their tops were often obscured by the crowns of nearby dominant trees, further complicating height estimation. These difficulties are particularly pronounced with European beech trees, characterized by their ovoid crowns within stands and high frequency of windings (Sofletea & Curtu 2007). Consequently, determining tree heights as local maxima from tree positions became unreliable when tree crowns interlocked. To address this, we opted to derive heights at the PSAlevel from the height of the tree bole (cylinder) calculated from TLS data. As such, we determined Hp50, Hstd, and Hp01, which we deemed suitable as input variables for the volume models. By utilizing the tree cylinder, which closely approximates actual tree height, we hypothesized that these may effectively capture competitive relationships between trees. Future research should explore integrating TLS with UAV-derived canopy models to improve height estimation accuracy. Additionally, validating these models in different forest types will enhance their robustness and applicability.

Other authors, like Yusup et al. (2023), tested 16 parametric (i.e. regression) models to estimate trunk volume (Vt) for Euphrates poplar trees using TLS data along the Tarim River, NW China. Sixteen regression models using the variables tree height, trunk height, under branch height, DBH, crown diameter, crown area, basal trunk diameter, were tested, one model performing best, accurately predicting Vt for irregularly shaped trees with 93.18% accuracy. All the trees were completely scanned with the TLS device and were generally distance to each other, thus the determination of their height from the point cloud point didn't pose significant challenges. The study concluded that TLS can effectively measure irregular trunk shapes of *Populus euphratica* and developed accurate Vt prediction models, suggesting multivariate models as more effective in prediction.

As previously mentioned, one of the main drawbacks in our study was the inability to directly measure the tree heights from the TLS data. This limitation may be alleviated by combining TLS data with other remote sensing technologies, complementary to each other. For instance, the tree heights may be obtained by combining a TLS derived terrain model with a canopy model extracted from UAV data, as performed by Iizuka et al. 2020.

## Conclusions

Considering the results obtained in the study regarding the application of parametric models to estimate tree stem volume, it was highlighted that DBH, when used as a single variable extracted from TLS data, accurately predicted the tree volumes.

A significant contribution of this study is the successful integration of variables extracted from TLS into a non-parametric model based on the RF algorithm.

This study demonstrates the efficacy of integrating TLS data with non-parametric models for accurate tree volume estimation.

The findings have significant implications for precision forestry, enabling better biomass estimation and forest management.

Further research should focus on extending these models to diverse forest ecosystems and integrating complementary remote sensing technologies.

## Acknowledgements

This research was made possible through the funding provided by the Romanian Ministry of Research, Innovation and Digitalization, FORCLIMSOC Nucleu Program (Contract 12N/2023), project PN 23090204 and project „Creșterea capacității și performanței instituționale a INCDS „Marin Drăcea" în activitatea de CDI - CresPerfInst" (Contract 34PFE/30.12.2021).

## References

Abegg M., Bösch R., Kükenbrink D., Morsdorf F., 2023. Tree volume estimation with terrestrial laser scanning — Testing for bias in a 3D virtual environment. Agricultural and Forest Meteorology 331: 109348 . https://doi.org/10.1016/j.agrformet.2023.109348

Aguilar F.J., Nemmaoui A., Aguilar M.A., Peñalver A., 2021. Building tree allometry relationships based on TLS point clouds and machine learning regression. Applied Sciences (Switzerland) 11(21): 10139. https://doi.org/10.3390/app112110139

Åkerblom M., Kaitaniemi P., 2021. Terrestrial laser scanning: A new standard of forest measuring and modelling? Annals of Botany 128(6): 653-662. https://doi.org/10.1093/aob/mcab111

Apostol B., Lorenţ A., Petrila M., Gancz V., Badea O., 2016. Height extraction and stand volume estimation based on fusion airborne LiDAR data and terrestrial measurements for a Norway spruce [*Picea abies* (L.) Karst.] test site in Romania. Notulae Botanicae Horti Agrobotanici Cluj-Napoca 44(1): 313-323. https://doi.org/10.15835/nbha44110155

Apostol B., Chivulescu S., Ciceu A., Petrila M., Pascu I.S., Apostol E.N., Leca Ş., Lorenţ A., Tănase M., Badea O., 2018. Data collection methods for forest inventory: A comparison between an integrated conventional equipament and terrestrial laser scanning. Annals of Forest Research 61(2): 189-202. https://doi.org/10.15287/afr.2018.1189

Auret L., Aldrich C., 2012. Interpretation of nonlinear relationships between process variables by use of random forests. Minerals Engineering, 35: 27–42. https://doi.org/10.1016/j.mineng.2012.05.008

Badea O., 2013. Cercetări ecologice pe termen scurt în ecosisteme forestiere reprezentative din Parcul Natural Bucegi. Seria II. Lucrări de cercetare. Ed. Silvică.

Bienert A., Georgi L., Kunz M., Maas H.G., von Oheimb G., 2018. Comparison and combination of mobile and terrestrial laser scanning for natural forest inventories. Forests 9(7): 395. https://doi.org/10.3390/f9070395

Bogdanovich E., Perez-Priego O., El-Madany T.S., Guderle M., Pacheco-Labrador J., Levick S.R., Moreno G., Carrara A., Pilar Martín M., Migliavacca M., 2021. Using terrestrial laser scanning for characterizing tree structural parameters and their changes under different management in a Mediterranean open woodland. Forest Ecology and Management 486: 118945. https://doi.org/10.1016/j.foreco.2021.118945

Brede B., Terryn L., Barbier N., Bartholomeus H.M., Bartolo R., Calders K., Derroire G., Krishna Moorthy S.M., Lau A., Levick S.R., Raumonen P., Verbeeck H., Wang D., Whiteside T., van der Zee J., Herold M., 2022. Non-destructive estimation of individual tree biomass: Allometric models, terrestrial and UAV laser scanning. Remote Sensing of Environment 280: 113180. https://doi.org/10.1016/j.rse.2022.113180

Burt A., Disney M.I., Raumonen P., Armston J., Calders K., Lewis P., 2013. Rapid characterisation of forest structure from TLS and 3D modelling. In: International Geoscience and Remote Sensing Symposium (IGARSS). 3387-3390. https://doi.org/10.1109/IGARSS.2013.6723555

Cabo C., Ordóñez C., López-Sánchez C.A., Armesto J., 2018. Automatic dendrometry: Tree detection, tree height and diameter estimation using terrestrial laser scanning. International Journal of Applied Earth Observation and Geoinformation 69: 164-174. https://doi.org/10.1016/j.jag.2018.01.011

Calders K., Adams J., Armston J., Bartholomeus H., Bauwens S., Bentley L.P., Chave J., Danson F.M., Demol M., Disney M., Gaulton R., Krishna Moorthy S.M., Levick S.R., Saarinen N., Schaaf C., Stovall A., Terryn L., Wilkes P., Verbeeck H., 2020. Terrestrial laser scanning in forest ecology: Expanding the horizon. Remote Sensing of Environment, 251: 112102. https://doi.org/10.1016/j.rse.2020.112102

Cojoacă FD, 2016. Management plan of Production Unit VI Cuntu, Experimental Base of Caransebeş, INCDS ”Marin Drăcea”.

de Conto T., Olofsson K., Görgens E.B., Rodriguez L.C.E., Almeida G., 2017. Performance of stem denoising and stem modelling algorithms on single tree point clouds from terrestrial laser scanning. Computers and Electronics in Agriculture 143: 165-176. https://doi.org/10.1016/j.compag.2017.10.019

Demol M., Calders K., Verbeeck H., Gielen B., 2021. Forest above-ground volume assessments with terrestrial laser scanning: A ground-truth validation experiment in temperate, managed forests. Annals of Botany 128(6): 805-819. https://doi.org/10.1093/aob/mcab110

Demol M., Verbeeck H., Gielen B., Armston J., Burt A., Disney M., Duncanson L., Hackenberg J., Kükenbrink D., Lau A., Ploton P., Sewdien A., Stovall A., Takoudjou S.M., Volkova L., Weston C., Wortel V., Calders K., 2022. Estimating forest above-ground biomass with terrestrial laser scanning: Current status and future directions. Methods in Ecology and Evolution. 13 (8). https://doi.org/10.1111/2041-210X.13906

Disney M., Burt A., Calders K., et al., 2019. Innovations in ground and airborne technologies as reference and for training and validation: Terrestrial Laser Scanning (TLS). Surv Geophys 40: 937-958. https://doi.org/10.1007/s10712-019-09527-x

Dobre A.C., Pascu I.S., Leca S., Garcia-Duro J., Dobrota C.E., Tudoran G.M., Badea O., 2021. Applications of tls and als in evaluating forest ecosystem services: A southern Carpathians case study. Forests 12(9): 1269. https://doi.org/10.3390/f12091269

Esteban J., McRoberts R.E., Fernández-Landa A., Tomé J.L., Næsset E., 2019. Estimating forest volume and biomass and their changes using random forests and remotely sensed data. Remote Sensing 11(16): 1944. https://doi.org/10.3390/rs11161944

Fardusi M.J., Chianucci F., Barbati A., 2017. Concept to practices of geospatial information tools to assist forest management and planning under precision forestry framework: a review. Annals of Silvicultural Research 41: 3–14

FARO Technologies Inc. 2019. FARO Laser Scanner Focus3D X130. User Manuals and Quick Start Guides for the Focus Laser Scanner.

García M., Danson F.M., Riaño D., Chuvieco E., Ramirez F.A., Bandugula V., 2011. Terrestrial laser scanning to estimate plot-level forest canopy fuel properties. International Journal of Applied Earth Observation and Geoinformation 13(4): 636-645. https://doi.org/10.1016/j.jag.2011.03.006

Giurgiu V., 1979. Dendrometrie și auxologie forestieră. Ed. Ceres, București.

Giurgiu V., Decei I., Draghiciu D., 2004. Metode și tabele dendrometrice. Ed. Ceres, București.

Han T., Sánchez-Azofeifa G.A., 2022. Extraction of Liana Stems Using Geometric Features from Terrestrial Laser Scanning Point Clouds. Remote Sensing 14(16): 4039. https://doi.org/10.3390/rs14164039

Hirigoyen A., Acosta-Muñoz C., Salamanca A.J.A., Varo-Martinez M.Á., Rachid-Casnati C., Franco J., Navarro-Cerrillo R., 2021. A machine learning approach to model leaf area index in *Eucalyptus plantations* using high-resolution satellite imagery and airborne laser scanner data. Annals of Forest Research 64(2):165-183. https://doi.org/10.15287/afr.2021.2073

Holopainen M., Vastaranta M., Hyyppä J., 2014. Outlook for the Next Generation's Precision Forestry in Finland. Forests 5(7): 1682–1694. https://doi.org/10.3390/f5071682

Hosingholizade A., Erfanifard Y., Alavipanah S.K., Latifi H., Jouybari-Moghaddam Y., 2023. Height estimation of pine (*Pinus eldarica*) single trees using slope corrected shadow length on unmanned aerial vehicle (UAV) imagery in a plantation forest. Annals of Forest Research 66(2): 3-16. https://doi.org/10.15287/afr.2023.3014

Iizuka K., Hayakawa Y.S., Ogura T., Nakata Y., Kosugi Y., Yonehara T., 2020. Integration of multi-sensor data to estimate plot-level stem volume using machine learning algorithms-case study of evergreen conifer planted forests in Japan. Remote Sensing 12(10): 1649. https://doi.org/10.3390/rs12101649

Lecigne B., Delagrange S., Messier C., 2018. Exploring trees in three dimensions: VoxR, a novel voxel-based R package dedicated to analysing the complex arrangement of tree crowns. Annals of Botany 121(4): 589-601. https://doi.org/10.1093/aob/mcx095

Li W., Niu Z., Shang R., Qin Y., Wang L., Chen H., 2020. High-resolution mapping of forest canopy height using machine learning by coupling ICESat-2 LiDAR with Sentinel-1, Sentinel-2 and Landsat-8 data. International Journal of Applied Earth Observation and Geoinformation 92: 102163. https://doi.org/10.1016/j.jag.2020.102163

Liang X., Litkey P., Hyyppä J., Kaartinen H., Vastaranta M., Holopainen M., 2012.Automatic stem mapping using single-scan terrestrial laser scanning. IEEE Trans. Geosci. Remote Sens. 50(2): 661-670. https://doi.org/10.1109/TGRS.2011.2161613

Liang X., Kankare V., Hyyppä J., Wang Y., Kukko A., Haggrén H., Yu X., Kaartinen H., Jaakkola A., Guan F., Holopainen M., Vastaranta M., 2016. Terrestrial laser scanning in forest inventories. ISPRS Journal of Photogrammetry and Remote Sensing 115: 63-77. https://doi.org/10.1016/j.isprsjprs.2016.01.006

Lim K., Treitz P., Wulder M., St-Ongé B., Flood M., 2003. LiDAR remote sensing of forest structure. Progress in Physical Geography 27(1): 88-106. https://doi.org/10.1191/0309133303pp360ra

Long S., Zeng S., Wang G., 2021. Developing a new model for predicting the diameter distribution of oak forests using an artificial neural network. Annals of Forest Research 64(2): 3-20. https://doi.org/10.15287/afr.2021.2060

Maas H.G., Bienert A., Scheller S., Keane E., 2008. Automatic forest inventory parameter determination from terrestrial laser scanner data. In: International Journal of Remote Sensing. 1579-1593. https://doi.org/10.1080/01431160701736406

Mayamanikandan T., Reddy R.S., Jha C.S., 2019. Non-Destructive Tree Volume Estimation using Terrestrial Lidar Data in Teak Dominated Central Indian Forests. In: Proceedings of the 2019 IEEE Recent Advances in Geoscience and Remote Sensing: Technologies, Standards and Applications, TENGARSS 2019. 100-103. https://doi.org/10.1109/TENGARSS48957.2019.8976068

Molina-Valero J.A., Martínez-Calvo A., Ginzo Villamayor M.J., Novo Pérez M.A., Álvarez-González J.G., Montes F., Pérez-Cruzado C., 2022. Operationalizing the use of TLS in forest inventories: The R package FORTLS. Environmental Modelling and Software 150: 105337. https://doi.org/10.1016/j.envsoft.2022.105337

Momo Takoudjou S., Ploton P., Sonké B., Hackenberg J., Griffon S., de Coligny F., Kamdem N.G., Libalah M., Mofack G., Le Moguédec G., Pélissier R., Barbier N., 2018. Using terrestrial laser scanning data to estimate large tropical trees biomass and calibrate allometric models: A comparison with traditional destructive approach. Methods in Ecology and Evolution 9(4): 905-916. https://doi.org/10.1111/2041-210X.12933

Moskal L.M., Zheng G., 2012. Retrieving forest inventory variables with terrestrial laser scanning (TLS) in urban heterogeneous forest. Remote Sensing 4(1): 1-20. https://doi.org/10.3390/rs4010001

Niță D.M., 2021. Testing forestry digital twinning workflow based on mobile LiDAR scanner and AI Platform. Forests 12(11): 1576. https://doi.org/10.3390/f12111576

Olofsson K., Holmgren J., Olsson H., 2014. Tree stem and height measurements using terrestrial laser scanning and the RANSAC algorithm. Remote Sensing 6(5): 4323-4344. https://doi.org/10.3390/rs6054323

Oruç M.E., Öztürk İ.L., 2021. Usability of terrestrial laser technique in forest management planning. Turkey Lidar Journal 3(1): 17-24. https://doi.org/10.51946/melid.922948

Pascu I.S., Dobre A.C., Badea O., Tănase M.A., 2019. Estimating forest stand structure attributes from terrestrial laser scans. Science of the Total Environment 691: 205-215. https://doi.org/10.1016/j.scitotenv.2019.06.536

Pascu I.S., Dobre A.C., Badea O., Tanase M.A., 2020. Retrieval of forest structural parameters from terrestrial laser scanning: A Romanian case study. Forests 11(4): 392. https://doi.org/10.3390/F11040392

Pascual C., Mauro F., Garcia-Abril A., Manzanera J.A., 2019. Applications of ALS (Airborne Laser Scanning) data to Forest Inventory. Experiences with pine stands from mountainous environments in Spain. In: IOP Conference Series: Earth and Environmental Science. 012001. https://doi.org/10.1088/1755-1315/226/1/012001

Petrila M., Apostol B., Lorenţ A., Gancz V., Silaghi D., 2012. Forest biomass estimation by the use of airborne laser scanning data and in situ FieldMap measurements in a spruce forest stand. Folia Forestalia Polonica, Series A 54(2): 84-93.

Pitkänen T.P., Raumonen P., Liang X., Lehtomäki M., Kangas A., 2021. Improving TLS-based stem volume estimates by field measurements. Computers and Electronics in Agriculture 180: 105882. https://doi.org/10.1016/j.compag.2020.105882

Popescu S.C., Wynne R.H., Nelson R.F., 2003. Measuring individual tree crown diameter with lidar and assessing its influence on estimating forest volume and biomass. Canadian Journal of Remote Sensing 29(5): 564-577. https://doi.org/10.5589/m03-027

R Core Team T., 2021. R: A language and environment for statistical computing v. 3.6. 1 (R Foundation for Statistical Computing, Vienna, Austria, 2019). Scientific Reports. 11.

Rehush N., Abegg M., Waser L.T., Brändli U.B., 2018. Identifying tree-related microhabitats in TLS point clouds using machine learning. Remote Sensing 10(11): 1735. https://doi.org/10.3390/rs10111735

Saarinen N., Kankare V., Vastaranta M., Luoma V., Pyörälä J., Tanhuanpää T., Liang X., Kaartinen H., Kukko A., Jaakkola A., Yu X., Holopainen M., Hyyppä J., 2017. Feasibility of Terrestrial laser scanning for collecting stem volume information from single trees. ISPRS Journal of Photogrammetry and Remote Sensing 123: 140-158. https://doi.org/10.1016/j.isprsjprs.2016.11.012

Schonlau M., and Zou R. Y., 2020. The random forest algorithm for statistical learning. SageJournals 20(1): 3-29. https://doi.org/10.1177/1536867X20909688

Shang C., Treitz P., Caspersen J., Jones T., 2019. Estimation of forest structural and compositional variables using ALS data and multi-seasonal satellite imagery. International Journal of Applied Earth Observation and Geoinformation 78: 360-371. https://doi.org/10.1016/j.jag.2018.10.002

Silva C.A., Klauberg C., Hudak A.T., Vierling L.A., Jaafar W.S.W.M., Mohan M., Garcia M., Ferraz A., Cardil A., Saatchi S., 2017. Predicting stem total and assortment volumes in an industrial *Pinus taeda* L. forest plantation using airborne laser scanning data and random forest. Forests 8(7): 254. https://doi.org/10.3390/f8070254

Singh A., Kushwaha S.K.P., Nandy S., Padalia H., 2022. An approach for tree volume estimation using RANSAC and RHT algorithms from TLS dataset. Applied Geomatics 14(4): 9–99. https://doi.org/10.1007/s12518-022-00471-x

Smreček R., Michnová Z., Sačkov I., Danihelová Z., Levická M., Tuček J., 2018. Determining basic forest stand characteristics using airborne laser scanning in mixed forest stands of central Europe. IForest 11(1): 181-188. https://doi.org/10.3832/ifor2520-010

Sofletea N., Curtu L., 2007. Dendrologie. Ed. Universității Transilvania din Brașov. 540p.

Srinivasan S., Popescu S.C., Eriksson M., Sheridan R.D., Ku N.W., 2015. Terrestrial laser scanning as an effective tool to retrieve tree level height, crown width, and stem diameter. Remote Sensing 7(2): 1877-1896. https://doi.org/10.3390/rs70201877

Stovall A.E.L., Vorster A., Anderson R., Evangelista P., 2023. Developing nondestructive species-specific tree allometry with terrestrial laser scanning. Methods in Ecology and Evolution 14(1): 280-290. https://doi.org/10.1111/2041-210X.14027

Wagers S., Castilla G., Filiatrault M., Sanchez-Azofeifa G.A., 2021. Using TLS-Measured Tree Attributes to Estimate Aboveground Biomass in Small Black Spruce Trees. Forests 12(11): 1521. https://doi.org/10.3390/f12111521

Wang D., Liang X., Mofack G.I., Martin-Ducup O., 2021. Individual tree extraction from terrestrial laser scanning data via graph pathing. Forest Ecosystems 8(1): 67. https://doi.org/10.1186/s40663-021-00340-w

Wang F., Sun Y., Jia W., Zhu W., Li D., Zhang X., Tang Y., Guo H., 2023. Development of Estimation Models for Individual Tree Aboveground Biomass Based on TLS-Derived Parameters. Forests 14(2): 351. https://doi.org/10.3390/f14020351

Wardius Y., Hein S., 2024. Terrestrial laser scanning vs. manual methods for assessing complex forest stand structure: a comparative analysis on plenter forests. European Journal of Forest Research 143: 635-649. https://doi.org/10.1007/s10342-023-01641-1

Wezyk P., Koziol K., Glista M., Pierzchalski M., 2007. Terrestrial laser scanning versus traditional forest inventory first results from the polish forests. In: ISPRS Workshop on Laser Scanning 2007 and SilviLaser 2007, Finland.

White J.C., Coops N.C., Wulder M.A., Vastaranta M., Hilker T., Tompalski P., 2016. Remote Sensing Technologies for Enhancing Forest Inventories: A Review. Canadian Journal of Remote Sensing 42(5): 619-641. https://doi.org/10.1080/07038992.2016.1207484

Wilson N., Bradstock R., Bedward M., 2021. Detecting the effects of logging and wildfire on forest fuel structure using terrestrial laser scanning (TLS). Forest Ecology and Management 488: 119037. https://doi.org/10.1016/j.foreco.2021.119037

Yrttimaa T., Luoma V., Saarinen N., Kankare V., Junttila S., Holopainen M., ... & Vastaranta M., 2022. Exploring tree growth allometry using two-date terrestrial laser scanning. Forest Ecology and Management, 518: 120303.https://doi.org/10.1016/j.foreco.2022.120303

Yusup A., Halik Ü., Keyimu M., Aishan T., Abliz A., Dilixiati B., Wei J., 2023. Trunk volume estimation of irregular shaped *Populus euphratica* riparian forest using TLS point cloud data and multivariate prediction models. Forest Ecosystems 10: 100082. https://doi.org/10.1016/j.fecs.2022.100082

Zhong L., Cheng L., Xu H., Wu Y., Chen Y., Li M., 2017. Segmentation of individual trees from TLS and MLS Data. IEEE Journal of Selected Topics in Applied Earth Observations and Remote Sensing 10(2): 774-787. https://doi.org/10.1109/JSTARS.2016.2565519

Zhou M., Li C., Li Z., Yu Z., Zhou X., 2023 a. Stratification of vertical canopy structure to improve estimation of forest inventory attributes using airborne LiDAR data in a large subtropical region of China. Annals of Forest Research 66(2): 101-120. https://doi.org/10.15287/afr.2023.3361

Zhou R., Sun H., Ma K., Tang J., Chen S., Fu L., Liu Q., 2023 b. Improving estimation of tree parameters by fusing als and tls point cloud data based on canopy gap shape feature points. Drones 7(8): 524. https://doi.org/10.3390/drones7080524

Zhu Z., Kleinn C., Nölke N., 2020. Towards tree green crown volume: A methodological approach using terrestrial laser scanning. Remote Sensing. 12 (11): 1841. https://doi.org/10.3390/rs12111841